



Estimating Travel Time Distribution under different Traffic conditions

Younes Guessous, Maurice Aron, Neila Bhourri, Simon Cohen

► To cite this version:

Younes Guessous, Maurice Aron, Neila Bhourri, Simon Cohen. Estimating Travel Time Distribution under different Traffic conditions. EWGT - Euro Working Group on Transportation, Jul 2014, Spain. 10p. hal-01056557

HAL Id: hal-01056557

<https://hal.science/hal-01056557>

Submitted on 20 Aug 2014

HAL is a multi-disciplinary open access archive for the deposit and dissemination of scientific research documents, whether they are published or not. The documents may come from teaching and research institutions in France or abroad, or from public or private research centers.

L'archive ouverte pluridisciplinaire **HAL**, est destinée au dépôt et à la diffusion de documents scientifiques de niveau recherche, publiés ou non, émanant des établissements d'enseignement et de recherche français ou étrangers, des laboratoires publics ou privés.

Estimating Travel Time Distribution under different Traffic conditions

Younes Guessous^a, Maurice Aron^{b*}, Neila Bhour^b, Simon Cohen^b

^a Ecole des Ponts-ParisTech, 6-8 avenue Blaise Pascal, Cité Descartes 77455 Champs sur Marne Cedex, France

^b IFSTTAR/COSYS/GRETTIA, 14-20 bd Newton 77447 Champs sur Marne Cedex, France

Abstract

Increasing mobility and congestion result in an increase in travel time variability and in a decrease in reliability. Reliability becomes an important performance measure for transportation facilities. A variety of performance measures have been proposed to quantify it. Many of these indicators are based on percentiles of travel time. The knowledge of the distribution of travel time is needed to properly estimate these values. Congestion distorts the distribution and particular statistical distributions are needed. Different distributions have been proposed in the literature. In a previous paper, we presented a comparison of six statistical distributions used to model travel time. These six distributions are the Lognormal, Gamma, Burr, Weibull, a mixture of two Normal distributions and a mixture of two Gamma distributions.

In this paper a probabilistic modeling of travel time which takes into account the levels-of-service is given. Levels of service are identified, then travel time distributions are modeled by level of service. This result in a very good fit between the empirical and modeled distributions. Moreover, the adjustment was improved, thanks to the calibration of “Bureau of Public Roads” functions, linking the travel time to the traffic flow by level of service.

The superiority of the Singh-Maddala distribution appears in many cases. This has been validated, thanks to travel time data from the same site at another period. However the parameters of the distributions vary from one year to another, due to changes in infrastructure. The transferability of the approach, not performed, will be based on travel time data on another site.

Keywords: congestion; traffic flow; travel time; motorway; modeling; statistics; reliability; distribution; Bureau of Public Roads.

1. Introduction

Traffic congestion impacts speed, thus travel time. When traffic increases and approaches the full capacity of the network, the flow becomes unstable and much more vulnerable to incidents, road works or bad weather. This increases the variability of travel time, to which users are very sensitive. Therefore, travel time reliability has become an important performance criterion for transportation facilities, complementing the traditional measures such as delay and average travel time. In recent research, a variety of performance measures have been proposed to quantify reliability and monetize it. This includes planning time, buffer time, standard deviation, coefficient of

* Corresponding author. Tel.: +33181668687.

E-mail address: maurice.aron@ifsttar.fr

variation, skewness,... - an overview is given in (Lomax, Schrank, Tyrmer & Margiotta, 2003). These indicators are based on percentiles of travel time. The knowledge of the travel time distribution is then needed.

Different distributions are presented in the literature as the best way to model the travel time distribution. (Richardson & Taylor, 1978), (Rakha, Shawarby, Arafeh & Dion, 2006), (Pu, 2010) and (Arezoumandi, 2011) concluded for a Lognormal distribution. Polus (1979) concluded for a Gamma distribution; however Al-Deek and Eman (2006) proposed a Weibull one. In (Taylor & Susilawati 2012) and (Susilawati et al., 2012) the Burr XII distribution is adopted, the advantage of this latter method is that its tails often fit the empirical ones. Aron, Bhouri and Guessous (2012) presented a comparison of six statistical distributions used to model travel time. Tests were conducted to identify the parameters of these different statistical distributions on the basis of real time data collected on a weaving section of the A4-A86 French urban motorway.

Based on the same data, this paper uses the Burr XII distribution, completed by a scale parameter introduced by Singh and Maddala (1976) to model travel time over five levels of service. The next section is dedicated to data collection. A method for levels-of-service extraction using the fundamental diagram is given in section 3. Calculation of the travel time and modeling of its distribution over five levels-of-service are presented in section 4. In section 5, the travel time distribution calibration is improved, using relations linking travel time to flow.

Nomenclature

i (resp.j)	index for lanes (resp. sections)
n (resp.m)	number of lanes (resp. sections)
q	traffic flow (number of vehicles per hour)
k	traffic density (number of vehicles per kilometre)
v	speed (kilometre/hour)

2. Data collection

The data used in this paper was collected on a weaving section of the A4-A86 French urban motorway. A two-lane urban motorway ring (A86) round Paris and a three-lane West-East urban motorway (A4) meet in the east of Paris and share a four-lane 2.3 km-long section. Traffic is particularly dense at some hours, and causes the greatest traffic bottleneck in Europe. Data used in this paper were collected in the year 2002, on a 3-km long stretch (2.3 on the weaving section, 0.7 km downstream), in the Eastbound direction. Four inductive loops (three on the weaving section, one downstream) provide every six minutes flow, occupancy and average speed by lane.

Although the data are generally very good, some are missing, inaccurate or irrelevant. A mean speed for one lane lower than 2 km/h or higher than 150 km/h, is considered as an outlier. Other anomalies in traffic data are identified – occupancy greater than 100% or 6-minute flow (by lane) greater than 400 vehicles. In these cases the data for the corresponding period and lane are cancelled and considered as missing. When this occurs in 2002, the missing data for a given period and lane is substituted, when possible, by data from a corresponding period from the year 2001 or 2000, the same day of the week, the same exact time and approximately the same date.

3. Level-Of-Service

3.1. Fundamental Diagram

The three macroscopic traffic variables - traffic flow q , traffic density k and average speed v - are linked by the equation $q=k.v$. Furthermore, when traffic density increases, speed decreases. This phenomenon is modeled by a

relation between speed and density (or flow), called “Fundamental Diagram”. An example of a fundamental diagram is provided in Figure 1. The first part of the graph represents the free flow, where the interaction between vehicles is light; then traffic flow increases along with traffic density until the critical density value k_c . Corresponding flow is the maximal flow q_{\max} sustained by the infrastructure. Above this density, vehicles are bunched and flow decreases. Flow is again equal to zero when density reaches its maximum.

Fundamental diagram is plotted on the basis of experimental data, and allows a better understanding of traffic.

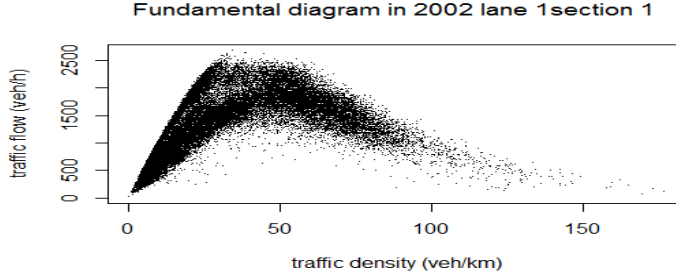


Fig. 1. Fundamental diagram in 2002 lane 1 section 1

3.2. Construction of a fundamental diagram for consecutive sections

In order to extract a simple information, the scatter plot is usually fit by a solid line. A division of this line in a few more homogeneous traffic states or "levels-of-service" is particularly useful.

So as to extract levels-of-service, we need first to construct a global fundamental diagram, since the data is presented by lanes ($i=1..n$) and section ($j=1..m$). Aggregation of speed, flow and density variables must be performed carefully to reflect reality, and the homogeneity of units must be thoroughly checked. We assert here that speed will be expressed in km/h, traffic flow in vehicles/hour and traffic density in vehicles/km.

Aggregation of data over lanes in one section is obtained by applying simple operations to the three traffic variables. We add traffic flows to obtain the flow for an entire section and we similarly add traffic densities. Speed for the entire section is the result of dividing the flow by the density. Formulas are the following:

$$q_j = \sum_{i=1}^n q_{ij} \quad ; \quad k_{ij} = \frac{q_{ij}}{v_{ij}} \quad \text{or} \quad \frac{1}{v_{ij}} = \frac{k_{ij}}{q_{ij}} \quad ; \quad k_j = \sum_{i=1}^n k_{ij} \quad \text{B} ; \quad \frac{1}{v_j} = \frac{\sum_{i=1}^n \left(\frac{k_{ij}}{q_{ij}} \right) \cdot q_{ij}}{\sum_{i=1}^n q_{ij}} = \frac{k_j}{q_j} \quad (1)$$

The last equation giving the harmonic average speed, weighted by traffic flows. Let L_j be the length and the travel time of section j , thus L_j/v_j is and its travel time. Travel times on consecutive sections being additive, the equation of the global average speed, on consecutive sections, is obtained by:

$$v = \sum_{j=1}^m L_j / \sum_{j=1}^m \frac{L_j}{v_j} ; \quad \text{As } N = \sum_{j=1}^m L_j k_j \text{ vehicles are present on the sections, thus the density is: } k = \sum_{j=1}^m L_j k_j / \sum_{j=1}^m L_j \quad (2)$$

$$\text{The global flow is the product of speed and density: } q = \frac{\sum_{j=1}^m L_j}{\sum_{j=1}^m \frac{L_j}{v_j}} \cdot \frac{\sum_{j=1}^m L_j k_j}{\sum_{j=1}^m L_j} = \frac{\sum_{j=1}^m L_j \frac{q_j}{v_j}}{\sum_{j=1}^m \frac{L_j}{v_j}} = \frac{\sum_{j=1}^m q_j \left(\frac{L_j}{v_j} \right)}{\sum_{j=1}^m \frac{L_j}{v_j}} \quad (3)$$

The flow is then the average of sections' flows weighted by travel times. It is also the total travel time (for all users) divided by the average travel time.

The global fundamental diagrams in 2002 and 2006 are shown in Figure 2(a) and 2(b). In 2006 points become less dense around 160 vehicles/km, whereas in 2002 they do so around 180 vehicles/km. That can be interpreted as the positive effect of opening hard shoulders to vehicles when congestion exceeds a certain level.

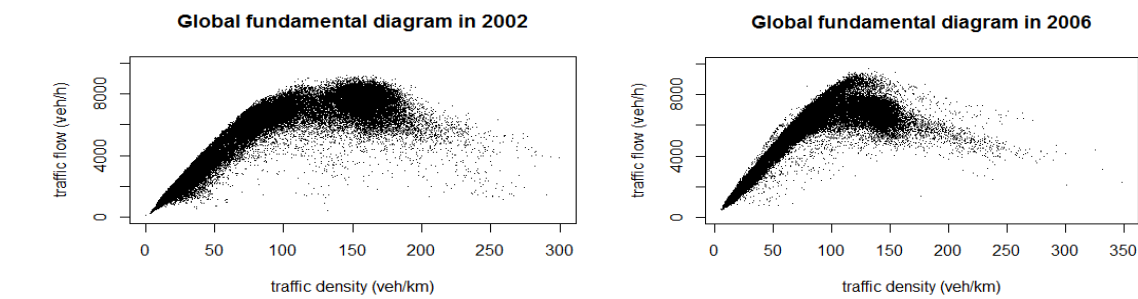


Figure 2 (a) Global fundamental diagram in 2002 (b) Global fundamental diagram in 2006 direction Paris to the East

3.3 Fitting the fundamental diagram

The levels of services are defined with respect to road capacity and critical density. Road capacity is not assumed to be the maximum observed traffic flow, which could be an outlier. Here road capacity is determined after fitting, in a first step an analytic curve to the scatter plot; the maximum of this curve gives the capacity.

Numerous models are used to fit the fundamental diagram. Some are summarized in Table 1 :

Table 1. Statistical models for fundamental diagrams

Model	Equation
Greenshields	$q=a*k+b*k^2$
Generalized power	$q=a*k+b*k^\alpha$
Underwood	$q=a*k*\exp(-b*k)$
Generalized exponential	$q=a*k*\exp(-b*k^\alpha)$

For each model we apply a nonlinear regression analysis, based on the least-square method - which provides acceptable results. All computations in this article are performed using R, an open-source statistical software.

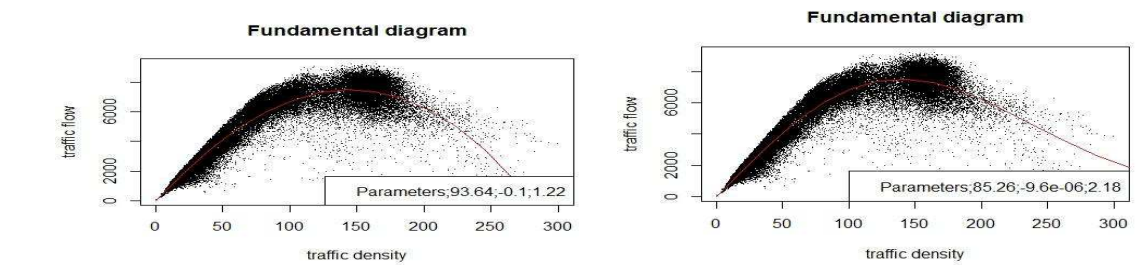


Figure 3. Global fundamental diagram in 2002 fitted with (a) a generalized power model (b) a generalized exponential model
Number of data: 53677; Residual standard error for (a) : 707.4 ; for (b) : 696.5

We compared only the generalized models. Figure 3 above and Figure 4 below show the adjustments of the generalized power and exponential models on the global fundamental diagram in 2002 and 2006.

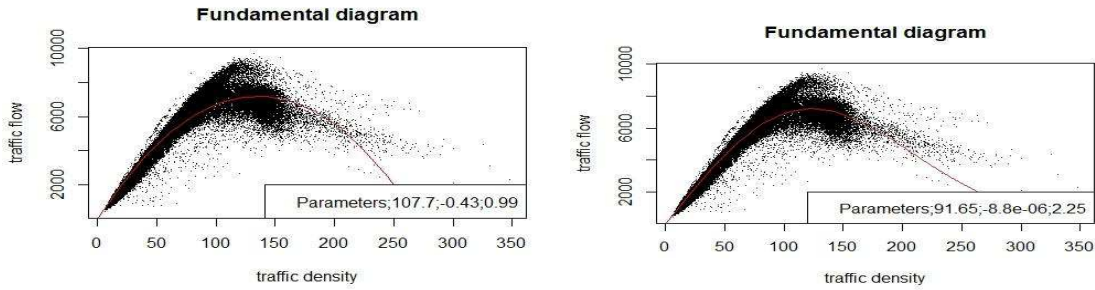


Figure 4. Global fundamental diagram in 2006 fitted with (a) a generalized power model (b) a generalized exponential model; Number of data: 53677; Residual standard error for (a) : 655; for (b) : 588.2

The Generalized Exponential, giving the best representation of the scatter plot's tail, is selected here.

3.4 Level-of-service computation

The road capacity and the critical density appear on the fitted fundamental diagram; separating the diagram in levels of service (LOS) is straightforward, using the LOS thresholds in terms of capacity percentage and density.

The six LOS defined by the High Capacity Manual are replaced in France by a simpler categorization of 4 LOS. In this article we are using customized five LOS which are defined as following:

- LOS 1 : density under critical density, and flow under 75% of capacity
- LOS 2 : density under critical density, and flow between 75% and 90% of capacity
- LOS 3 : density under critical density, and flow above 90 % of capacity
- LOS 4: density above critical density, and flow above 90% of capacity
- LOS 5: density above critical density, and flow under 90% of capacity

Four points separate the five LOS. Point 1 (between LOS 5 and 4); point 2 (between LOS 4 and 3); point 3 (between LOS 3 and 2); and point 4 (between LOS 2 and 1). Their flow, density and speed are given in Table 2.

Table 2. Flow, density and speed at four points separating the five LOS for 2002 and 2006

Points	2002			2006		
	Flow	Density	Speed	Flow	Density	Speed
1	6753.8	184.0	36.7	6497.2	161.6	40.2
2	7504.2	139.2	53.9	7219.1	122.8	58.8
3	6753.8	98.0	68.9	6497.2	86.9	74.7
4	5628.2	74.1	75.9	5414.3	65.9	82.1

4. Modeling travel time distribution by Level_Of-Service

Figure 5(a) and 5(b) show the placing of the five LOS and of the four separating points. Furthermore, in Figure 6 are displayed the travel time histograms by LOS; these are useful to select the distributions required for modeling.

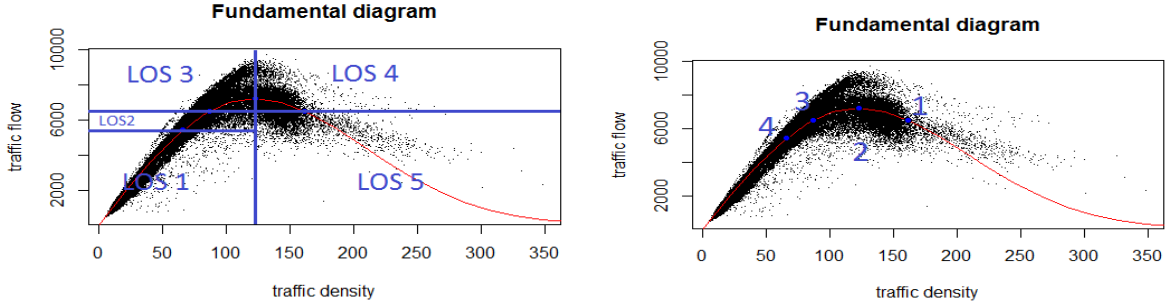


Fig. 5. (a) Levels-of-service selection (b) Computed points

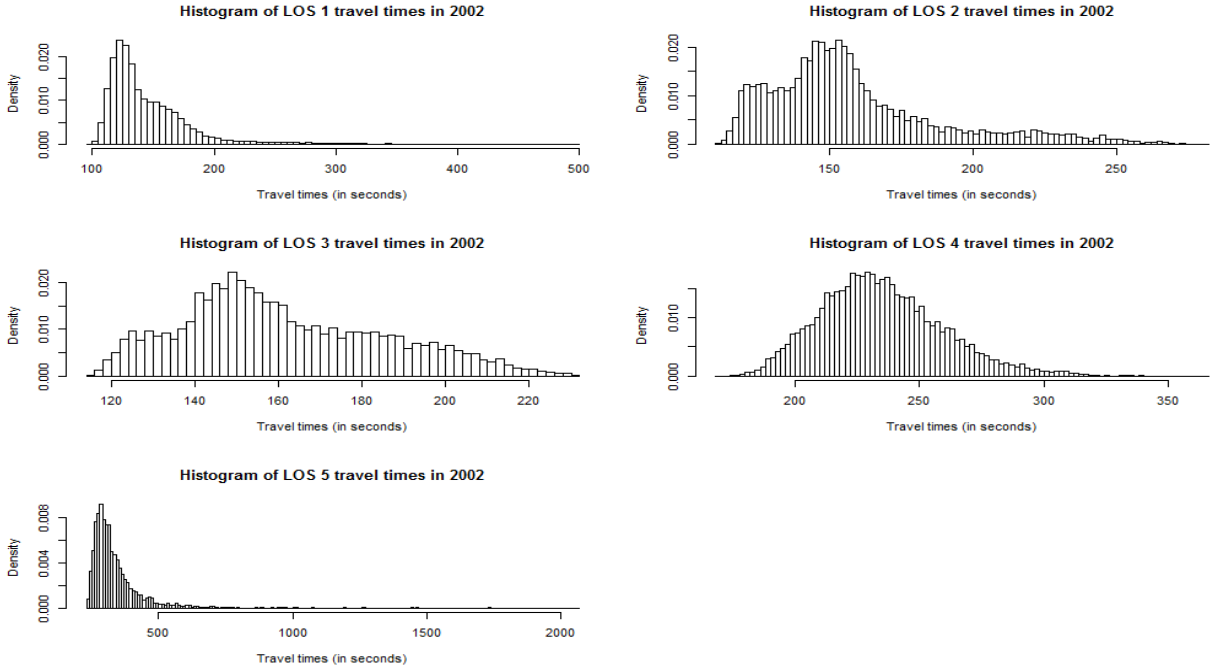


Fig. 6. Histogram of travel times separated by LOS in 2002

The likelihood of the lognormal and Singh-Maddala distributions are maximized on each LOS histogram.. The cumulative density function $F(x)$ and the probability density function $f(x)$ of the Singh-Maddala distribution are given below; any Singh-Maddala percentile $P(\alpha)$ of range α (α between 0% and 100%) derived by inverting $F(x)$;

$$\text{For } x > 0: F(x) = 1 - [1 + (x/b)^a]^{-q} ; f(x) = a \cdot (q/b) \cdot [1 + (x/b)^a]^{-q+1} ; P(\alpha) = b \cdot \sqrt[q]{(1 - \alpha)^{-1/q} - 1} \quad (4)$$

The 1st and 3rd parameters, a & q are shape parameters, whereas the second parameter b is a scale parameter. For the first to three LOS, a normal mixture model is also fitted. We evaluate the quality of the models by using

the Akaike information criterion (AIC), and select the model that minimizes this criterion (Table 3).

Table 3. AIC for the five LOS and three distribution models in 2002 (best distribution highlighted)

LOS	Number of data	Singh-Maddala	Lognormal	Normal mixture
1	24036	221876.36	230326.73	227150.70 (with 2 components)
2	7878	73971.82	74746.84	73530.72 (with 2 components)
3	6599	60821.46	60512.36	59872.96 (with 3 components)
4	10989	101480.51	101325.77	Not performed
5	4144	46622.16	49089.62	Not performed

LOS 3, 4 and 5, are the most interesting ones, because they occur near capacity or in congestion. Their adjustments to the models are presented here. Adjustments with a normal mixture have not been performed for LOS 4 and 5 because the empirical histograms have a single mode.

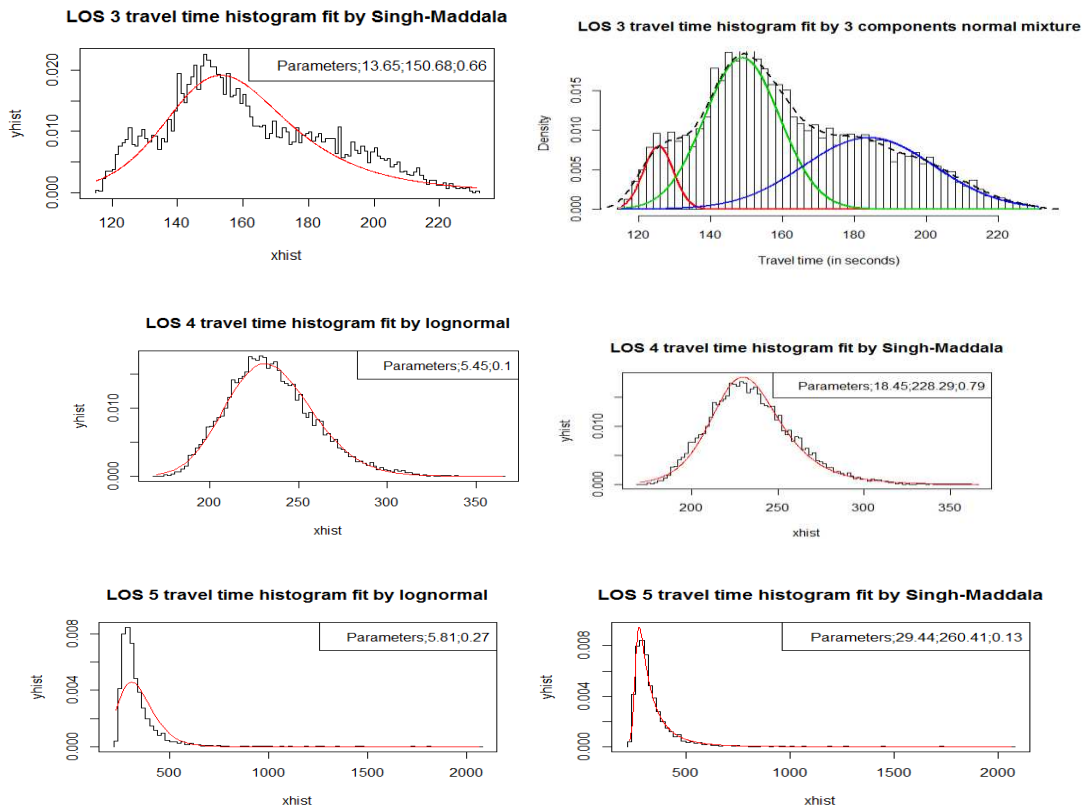


Fig. 7. Histogram of LOS 3, 4 and 5 travel times fit by different distributions in 2002

For LOS 3, three modes appear, and normal mixture outperforms Singh-Maddala.

For LOS 4, the AIC for the lognormal distribution is better than the one for the Singh-Maddala. However, the difference in this criterion between lognormal and Singh-Maddala is not significant enough compared to the same difference in LOS 3. Besides, we do not notice any significant difference graphically.

For LOS 5, Singh-Maddala outperforms the lognormal distribution from the AIC and graphics points of view.

With the AIC, the superiority of the Singh-Maddala distribution is confirmed from 2006 data for LOS 1, 4, 5, whereas it is lightly outperformed by normal mixture in LOS 2 and 3 (Table 4). The lognormal distribution lags far behind Singh-Maddala and normal mixture, except for LOS 4 where it is close to Singh-Maddala.

Table 4. Akaike information criterion for the five LOS and three distribution models in 2006

LOS	Number of data	Singh-Maddala	Lognormal	Normal mixture
1	23816	165571.60	178098.76	166346.62 (with 2 components)
2	9508	73814.98	78407.83	73757.59 (with 2 components)
3	10306	79115.66	82729.76	78913.22 (with 2 components)
4	6248	56111.66	56284.97	Not performed
5	3760	39100.80	40434.25	Not performed

Table 5 provides estimates for Singh-Maddala parameters in 2002 (and in parenthesis for 2006, LOS 1 only).

Table 5. Estimates and confidence intervals for Singh-Maddala parameters (five LOS in 2002 and LOS 1 in 2006)

LOS	Parameter	Lower bound	Estimate	Upper bound
1	shape1.a	31.98 (47.87)	32.01 (47.90)	32.05(47.92)
	Scale (in seconds)	115.65 (108.63)	115.65 (108.63)	115.65 (108.63)
	Shape 3 <i>q</i>	0.11 (0.27)	0.15 (0.31)	0.19 (0.34)
2	shape1.a	16.49	16.53	16.57
	Scale (in seconds)	136.31	136.32	136.33
	Shape 3 <i>q</i>	0.31	0.38	0.44
3	shape1.a	13.61	13.65	13.69
	Scale (in seconds)	150.67	150.68	150.69
	Shape 3 <i>q</i>	0.58	0.66	0.74
4	shape1.a	18.42	18.45	18.48
	Scale (in seconds)	228.28	228.29	228.29
	Shape 3 <i>q</i>	0.73	0.79	0.85
5	shape1.a	29.35	29.44	29.52
	Scale (in seconds)	260.40	260.41	260.42
	Shape 3 <i>q</i>	0.03	0.13	24

Let us recall that Singh-Maddala distribution has 3 parameters, while a normal mixture with 2 components has 2×2=4 parameters. We recommend using Singh-Maddala distribution: it is the most stable distribution and adapts to various levels-of-service. It provides a good trade-off between fitting quality and model simplicity.

However the numerical values obtained for the Singh-Maddala parameters are not validated: 2006 values (given in Table 5 for the first LOS) differ from 2002 values -. This is probably due to changes in infrastructure.

5. Improving travel time models

One way to improve travel time prediction is to find a relationship between travel time and flow. The Bureau of Public Roads (BPR) function (here applied by LOS) is the most used formula in this case:

$$T_l = T_0 \left(1 + \alpha \cdot \left(\frac{q_l}{q_{\max}} \right)^\beta \right)$$

Where ($l=1..5$) represents the LOS number. α and β are dimensionless parameters; their values and the quality of the regressions (in terms of p-value and residual standard error) are presented in Table 7.

Table 7. Statistical information for the 5 LOS in 2002

LOS	Number of data	Residual standard error (seconds)	α		β	
			estimate	p-value	Estimate	p-value
1	24036	76.61	1.419	<2e-16	0.454	<2e-16
2	7878	30.46	0.871	<2e-16	0.005	0.87
3	6599	24.32	0.926	<2e-16	0.135	7.06e-05
4	10989	24.21	1.750	<2e-16	-0.255	<2e-16
5	4144	139.4	2.606	<2e-16	-0.832	<2e-16

As p-values are below 0.05 (except for LOS 2), the BPR functions, relating travel time and traffic flow are significant for LOS 1, 3, 4 and 5. Residual standard errors are generally acceptable (see Table 7), given the facts that in free-flow (LOS 1) the speed is not constrained by the flow, and that by high congestion (LOS 5) the relation between travel time and flow vanishes. Non-linear regressions are illustrated for LOS 3 & 5 in Figure 8.

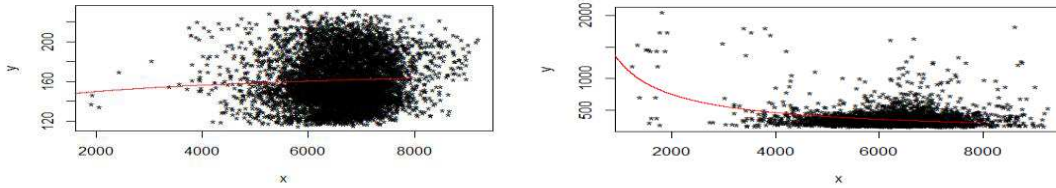


Figure 8. Non-linear regression between travel times (variable y) and flows (x) in 2002 for (a) LOS 3 (b) LOS 5

Then, applying the BPR functions on every travel time, we obtain a new “adapted” travel times series, more homogeneous, making possible a better adjustment. This happened. The improvement is very impressive for AIC values (Table 8). Due to the travel time queue, the slightest improvement is for LOS 5. The improvement remains slightly visible graphically for this LOS - see Figure 9, providing the original and adapted Singh-Maddala fits.

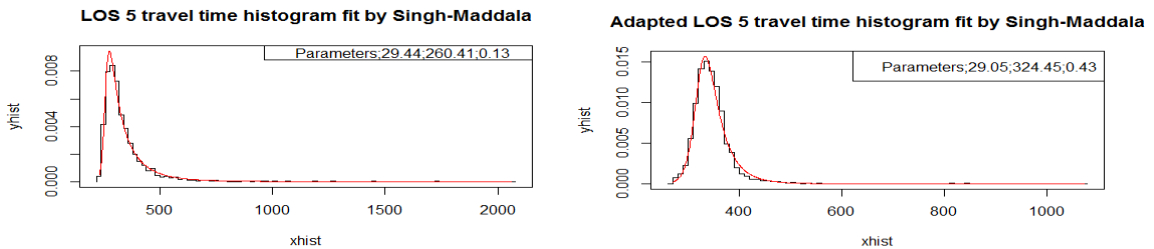


Figure 9. Histogram of original and adapted LOS 5 travel times fit by Singh-Maddala distribution in 2002

Table 8. AIC values for the five LOS travel times (originals and adapted) fit by Singh-Maddala in 2002

LOS	Number of data	Original	Adapted
1	24036	221876.36	134976
2	7878	73971.82	24641.99
3	6599	60821.46	20289.9
4	10989	101480.51	66013.44
5	4144	46622.16	40341.57

6. Conclusion

Basing reliability on *aggregated* travel times (here on 6-minute periods) and not on individual travel times is justified because it bases the information which is presented to users and which is taken into account in economics studies. The passage by *Levels-Of-Service* is now widespread in traffic studies because the homogeneity of a LOS induces more accurate treatments - this is confirmed here. The *Singh-Maddala* distribution is both appropriate (given the quality of the fit) and practical (for deriving percentiles, which are used in the reliability indicators). The use of BPR functions relating travel time to traffic flow (by LOS) improves the adjustments. However the numerical values of the parameters were not stable from one year to another, due to changes in the infrastructure. All of this contributes to a better understanding of travel time and of its reliability.

Acknowledgements

This work has been done with the support of Ecole des Ponts-ParisTech.

References

- Lomax, T., Schrank, D., Tyrmer, S. & Margiotta, R. (2003). Report of Selecting Travel Reliability Measures. <http://www.verkeerskunde.nl/reistijdbetrouwbaarheidsmodel/Verkeerskunde>. Texas Transportation Institute. Texas, USA.
- Richardson A. J. and Taylor, M.A.P. (1978). Travel time variability on commuter journeys. *High Speed Ground Transportation Journal*. 6. pp. 77–79.
- Rakha, H., El-Shawarby, I., M. Arafeh & Dion, F. (2006). Estimating Path Travel-Time Reliability. In Proceedings of the IEEE-ITSC 2006. Toronto, Canada. September 17–20.
- Pu, W. (2010). Analytic relationships between travel time reliability measures. Compendium of Papers TRB 90th Annual Meeting. Washington, D.C., USA.
- Arezoumandi, M. (2011). Estimation of Travel Time Reliability for Freeways Using Mean and Standard Deviation of Travel Time. *Journal of Transp. Syst. Engineering and Info. Tech.* Volume 11. Issue 6.
- Polus, A. (1979). A study of travel time and reliability on arterial routes. *Transportation*. 8. pp. 141–151.
- Al-Deek, H. & Emam, E.B. (2006). New methodology for estimating reliability in transportation networks with degraded link capacities. *Journal of Intelligent Transportation Systems*. pp. 117–129.
- Taylor, M. & Susilawati, S. (2012). Modeling travel time reliability with the Burr distribution. *Procedia - Social and Behavioral Sciences*. Volume 54. 4 October 2012. pp. 75–83.
- Susilawati, S., Taylor, M.A.P. & Somenahalli, S.V.C. (2012). Distributions of travel time variability on urban roads. *Journal of Advanced Transportation*. doi: <http://dx.doi.org/10.1002/atr.192>
- Bhouri, N., Aron, M. & Kauppila, J. (2012). Relevance of Travel Time Reliability Indicators: A Managed Lanes Case Study Original Research. *Procedia - Social and Behavioral Sciences*, Volume 54, 4 October, Pages 450-459. <http://www.sciencedirect.com/science/article/pii/S1877042812042255>
- Aron M., Bhouri N. and Guessous Y. (2014). "Estimating Travel Time Distribution for Reliability Analysis". Transport Research Arena 2014 Paris La Défense (France).
- Singh, S.K. and Maddala, G.S. (1976). A function for the size distribution of income. *Econometrika* 44; 963-970.